DYNAMIC RESPONSE OF AN UNDERGROUND TUNNEL TO SEISMIC WAVES

S.A. BADSAR[1] and M.A. ALIBAKHSHI[2]

[1] *Department of Civil Engineering, K.U. Leuven, Kasteelpark Arenberg 40, BE-3001 Leuven, Belgium. sayedali.badsar@bwk.kuleuven.be*
[2] *Iran University of Science and Technology, Narmak, Tehran 16844, Iran.*

(Received November 26, 2007; revised version accepted December 30, 2008)

ABSTRACT

Badsar, S.A. and Alibakhshi, M.A., 2009. Dynamic response of an underground tunnel to seismic waves. *Journal of Seismic Exploration*, 18: 181-198.

This study investigates the interaction of seismic waves with a cylindrical tunnel cavity embedded in a semi-infinite poroelastic medium. When seismic waves scatter from an underground tunnel, the magnitude and location of maximum tangential stresses on the tunnel cavity varies upon angle, frequency, and kind of the incident wave. The overburden thickness (depth of the tunnel) and the bulk properties of the surrounding medium also affect the response of such systems to dynamic excitations. Using Graf's addition theorem for the cylindrical Hankel functions, the multiple-scattering between the tunnel wall and the free surface is expressed in form of infinite series. To model the underground medium, the Biot dynamic model of poroelasticity is employed.

A crossover frequency f_x at which the wavelengths become comparable to the size of the tunnel, the Biot critical frequency, and the crossover frequency at which fluid diffusion length is of the order of the tunnel size are introduced. Results are discussed at the crossover frequency f_x. It is shown in this paper that neglecting the effect of the free boundary or using equivalent effective elastic medium approximations may lead to significant errors. A limiting case involving an elastic halfspace containing a long cylindrical cavity is considered and fair agreement with a previous study is established.

KEY WORDS: wave-induced damage, earthquake analysis, overburden thickness, poroelasticity, closed form solution, addition theorem.

0963-0651/09/$5.00

INTRODUCTION

Soil-structure interaction in the underground is a complex phenomenon, involving (multi) scattering and diffraction of the incident waves from the structure as well as the ground surface, and propagation of wave energy into the structure and radiation back into the soil. In this process, the soil, the ground surface and the structure, all are excited. To reduce the complexity of the problem, various simplifying assumptions have been made in previous studies, starting from ignoring the ground surface effect, the equivalent effective elastic medium approximations of poroelastic soil medium, and the wave nature of the excitation.

Using the series of Bessel function expansions, Lee et al. (1989) and Davis (2001) investigated the scattering and diffraction of plane SV-waves by circular cylindrical canyons and underground circular cylindrical cavities at various depths in an elastic half space. Using the same method, the scattering and diffraction of plane (P) waves by a circular canyon with variable width-to-depth ratio later on studied by Cao and Lee (1990). The dynamic problem of steady-state oscillations of a half space with different types of cylindrical inhomogeneities studied by Nazarenko (1991) afterwards. By an indirect boundary integral solution and based on a two-dimensional Green's function for a viscoelastic half-space, Luco and De Barros (1994) investigated the two-dimensional response of a viscoelastic half-space containing a buried, unlined, infinitely long cylindrical cavity of circular cross-section. An extensive critical review of the existing numerical results obtained by other techniques is also presented in the latter study. Filshtinsky and Bardzokas (2001) considered the antiplane steady dynamic problem of the theory of elasticity for an isotropic layer and a half-layer weakened by tunnel cavities of arbitrary cross section where a radiating monochromatic shear wave (SH-wave) is considered as loading. Subsequently, Chen et al. (2003) using the complex function method, constructed the Green's function of the dynamic stress concentration and scattering of SH-waves by bi-material structures.

However, the influence of slow waves and the overburden thickness on the mechanical properties of an underground structure have not been clarified yet, therefore, in this contribution, the dynamic behavior of a uniformly unlined tunnel located close to a free surface, subjected to P and SV-waves is investigated based on a two-dimensional linear elastic wave analysis.

FORMULATION

Before proceeding to analyze the full problem, we shall first review features of Biot's dynamic theory of poroelasticity. In the Biot model, the medium is taken to be a macroscopically homogeneous and isotropic

two-component solid-fluid system. It is therefore described in terms of averaged parameters. Denoting the average macroscopic displacement of the solid frame and the saturating fluid on the elementary macroscopic volume by the vectors **u** and **U**, respectively, the macroscopic stress tensor σ_{ij} and the mean pore fluid pressure p_p are given by (Bourbie et al., 1987):

$$\sigma_{ij} = (\lambda_f e - \beta M \xi)\delta_{ij} + 2\mu e_{ij} \quad , \quad p_p = M(\xi - \beta e) \tag{1}$$

where

$$\lambda_f = K_f - (2/3)\mu \quad ,$$

$$K_f = \{\phi_0[(1/K_s) - (1/K_{fl})] + (1/K_s) - (1/K_o)\}$$

$$/\{\phi_0/K_o[(1/K_s) - (1/K_{fl})] + 1/K_s[(1/K_s) - (1/K_o)]\} \quad ,$$

$$M = 1/[(\beta - \phi_0)/K + (\phi_0)/K_{fl})] \quad ,$$

$$\beta = 1 - K_o/K_s \quad , \quad e_{ij} = (u_{i,j} + u_{j,i})/2 \quad ,$$

$$\xi = -\nabla\cdot\mathbf{w} = -\phi_0(\epsilon - e) \quad , \quad e = \nabla\cdot\mathbf{u} \quad , \quad \epsilon = \nabla\cdot\mathbf{U} \quad , \tag{2}$$

in which $\mathbf{w} = \phi_0(\mathbf{U} - \mathbf{u})$ is the filtration displacement vector, ϕ_0 is the pore volume fraction (porosity), λ_f is the first Lamé coefficient for a "closed" system (i.e., for $\xi = 0$), K_f is the bulk modulus of the "closed" system, μ is the shear modulus of the bare skeletal frame, K_s is the bulk modulus of the material constituting the elastic matrix, K_{fl} is the bulk modulus of the saturating fluid, K_o is the bulk modulus of the dry skeleton (i.e., for the "open" system, $p_p = 0$), and e_{ij} is the macroscopic strain tensor. Also, the equations of motion governing the displacements of the solid matrix and interstitial liquid with dissipation taken into account are written as (Bourbie et al., 1987):

$$(\lambda + \mu)\nabla\nabla\cdot\mathbf{u} + Q\nabla\nabla\cdot\mathbf{U} - \nabla\times\nabla\times\mathbf{u} = \rho_{11}\ddot{\mathbf{u}} + \rho_{12}\ddot{\mathbf{U}} + b(\dot{\mathbf{u}} - \dot{\mathbf{U}}) \quad ,$$

$$Q\nabla\nabla\cdot\mathbf{u} + R\nabla\nabla\mathbf{U} = \rho_{12}\ddot{\mathbf{u}} + \rho_{22}\ddot{\mathbf{U}} - b(\dot{\mathbf{u}} - \dot{\mathbf{U}}) \quad , \tag{3}$$

where

$$\lambda = \lambda_f + \phi_0 M(\phi_0 - 2\beta) \quad ,$$

$$Q = \phi_0 M(\beta - \phi_0) \quad ,$$

$$R = \phi_0^2 M \quad ,$$

$$\rho = (1 - \phi_0)\rho_s + \phi_0\rho_{fl} \quad ,$$

$$\rho_{11} = \rho + \phi_0\rho_{fl}(\alpha_\infty - 2) \quad ,$$

$$\rho_{12} = \phi_0\rho_{fl}(1 - \alpha_\infty) \quad ,$$

$$\rho_{22} = \rho - \rho_{11} - 2\rho_{12} = \alpha_\infty\phi_0\rho_{fl} \quad . \tag{4}$$

where ρ_{11}, ρ_{12}, ρ_{22} are effective densities, which describe the combined effects of viscous and inertial drag, ρ_{fl} is the density of the saturating fluid, and α_∞ is the tortuosity (structure factor) of the porous medium. The quantity $b(\omega) = \phi_0^2\eta F(\omega)/\kappa$ is a viscous coupling factor that accounts for the combined effects of macroscopic frictional dissipation due to finite fluid viscosity (viscous drag forces) and the interaction between the fluid and solid movements (Allard, 1993), ω is the frequency of incident wave, η is the saturating fluid viscosity, and ω is the absolute (dc) permeability of a porous medium. According to Allard (1993), the simplest possible model for $F(\omega)$ is:

$$F(\omega) = [1 - j(4\alpha_\infty^2\kappa^2\rho_{fl}\omega)/(\eta\Lambda^2\phi_0^2)]^{1/2} \quad , \tag{5}$$

where $\Lambda = \sqrt{(8\alpha_\infty\kappa/\phi_0)}$ is the viscous characteristic length.

The Helmholtz decomposition allows us to resolve the displacement fields as superposition of longitudinal and transverse vector components:

$$\mathbf{u} = \nabla\phi + \nabla\times\psi \quad ,$$

$$\mathbf{U} = \nabla\chi + \nabla\times\Theta \quad .$$

Substituting the above resolutions into Biot's field equations of motion (3), we obtain two sets of coupled equations ($e^{-i\omega t}$ dependence suppressed for simplicity):

$$\nabla^2\phi_{f,s} + k_{f,s}^2\phi_{f,s} = 0 \quad ,$$

$$\nabla^2\psi + k_t^2\psi = 0 \quad , \tag{6}$$

where k_f, k_s and k_t which designate the complex wave numbers of the fast compressional, slow compressional, and the elastic shear waves, respectively, are given as

$$k_{f,s}^2 = [B \mp \sqrt{(B^2 - 4AC)}]/2A \quad , \quad k_t^2 = C/[\mu(\rho_{22}\omega^2 + i\omega b)] \quad , \tag{7}$$

where

$$A = (\lambda + 2\mu)R - Q^2 \quad ,$$

$$B = \omega^2[\rho_{11}R + \rho_{22}(\lambda + 2\mu) - 2\rho_{12}Q] + j\omega b(\lambda + 2\mu + 2Q + R)$$

$$C = \omega^2[\omega^2(\rho_{11}\rho_{22} - \rho_{12}^2) + j\omega\rho b] \quad . \tag{8}$$

Employing eqs. (6) and (7), with some manipulations, the scalar potentials ϕ, χ, Θ, and ψ may be expressed as:

$$\phi = \phi_f + \phi_s \quad ,$$

$$\chi = \mu_f\phi_f + \mu_s\phi_s \quad ,$$

$$\Theta = \alpha_0\psi \quad , \tag{9}$$

where

$$\mu_{f,s} = \{\omega^2(\rho_{11}R - \rho_{22}Q) - k_{f,s}^2[(\lambda + 2\mu)R - Q^2] + i\omega b(Q + R)\}$$

$$/\{\omega^2(\rho_{22}Q - \rho_{12}R) + j\omega b(Q + R)\} \quad . \tag{10}$$

$$\alpha_0 = -(\omega^2\rho_{12} - i\omega b)/(\omega^2\rho_{22} + i\omega b) \quad . \tag{11}$$

The problem we will consider has the geometry illustrated in Fig. 1. Two different cases for incident wave are considered. The incident wave may be a plane fast compressional wave or a plane vertical shear wave, and has the form:

$$\phi_{inc} = e^{ik_{inc}r_i\cos(\theta_i - \alpha)} \quad ; \quad k_{inc} = k_f, k_i \tag{12}$$

with i = 1,2 corresponding to the first and second cylinder, respectively, and α is the angle of incidence. We may specify (12) as a series with known coefficients, using the plane wave representation in the cylindrical coordinate system of each cylindrical cavity given by Morse and Feshbach (1953):

$$\phi_{inc}^{(i)} = \sum_{n=0}^{\infty} \Omega_n^{(i)} J_n(k_{inc}r_i)e^{in\theta_i} \quad , \quad \Omega_n^{(1)} = i^n e^{-in\alpha}, \quad \Omega_n^{(2)} = \Omega_n^{(1)} e^{ik_{inc}d\cos\alpha} \tag{13}$$

where J_n is the cylindrical Bessel function of the first kind (Abramovitz and Stegun, 1964) and d is the distance between the axes of the two cylinders. Last, the field expansions for the fast dilatational wave, the slow dilatational wave, and the shear wave scattered by each cylindrical cavity in poroelastic medium may be expressed in the general form:

$$\phi_f^{(i)} = \sum_{n=-\infty}^{\infty} A_n^{(i)} H_n(k_f r_i)e^{in\theta_i} \quad ,$$

$$\phi_s^{(i)} = \sum_{n=-\infty}^{\infty} B_n^{(i)} H_n(k_s r_i) e^{in\theta_i} \quad ,$$

$$\phi_t^{(i)} = \sum_{n=-\infty}^{\infty} C_n^{(i)} H_n(k_t r_i) e^{in\theta_i} \quad , \tag{14}$$

where H_n is the Hankel function of the first kind introduced in order to respect the radiation condition of Sommerfeld (Abramovitz and Stegun, 1964). The coefficients $A_n^{(i)}$, $B_n^{(i)}$ and $C_n^{(i)}$ are unknown complex numbers which must be determined so as to satisfy boundary conditions on the surface of each cylinder where i = 1,2 corresponding to the first and the second cylinder, respectively.

Now considering the fundamental field equations in the general cylindrical coordinate, the solid and the liquid displacement in r- and θ-directions in terms of displacement potentials for a poroelastic medium are written as (Achenbach, 1973):

$$u_r = (\partial\phi/\partial r) + (1/r)(\partial\psi/\partial\theta) \quad , \quad u_\theta = (1/r)(\partial\phi/\partial\theta) - (\partial\psi/\partial r) \quad ,$$

$$U_r = (\partial\chi/\partial r) + (1/r)(\partial\Theta/\partial\theta) \quad , \quad u_\theta = (1/r)(\partial\chi/\partial\theta) - (\partial\Theta/\partial r) \quad . \tag{15}$$

Expressions for the frame and the liquid dilatations can be manipulated to yield:

$$e = \nabla\cdot\mathbf{u} = \nabla^2\phi = \nabla^2\phi_f + \nabla^2\phi_s = -k_f^2\phi_f - k_s^2\phi_s \quad ,$$

$$\epsilon = \nabla\cdot\mathbf{U} = \nabla^2\chi = \mu_f\nabla^2\phi_f + \mu_s\nabla^2\phi_s = -\mu_f k_f^2\phi_f - \mu_s k_s^2\phi_s \quad . \tag{16}$$

Utilizing eqs. (1), (9), (15), and (16), the pore fluid pressure, the radial and tangential stress components are expressed as:

$$\sigma_{rr} = a_f k_f^2\phi_f + a_s k_s^2\phi_s + 2\mu(\partial u_r/\partial r) \quad ,$$

$$p_p = Mb_f k_f^2\phi_f + Mb_s k_s^2\phi_s \quad ,$$

$$\sigma_{r\theta} = (\mu/r)[(\partial u_r/\partial\theta) + r(\partial u_\theta/\partial r) - u_\theta] \quad ,$$

$$\sigma_{\theta\theta} = (\lambda_f e - \beta M\zeta) + 2\mu[(u_r/r) + (\partial u_\theta/r\partial\theta)] \quad , \tag{17}$$

where

$$a_{f,s} = -\lambda_f + \phi_0\beta M(1 - \mu_{f,s}) \quad ,$$

$$b_{f,s} = \beta + \phi_0(\mu_{f,s} - 1) \quad .$$

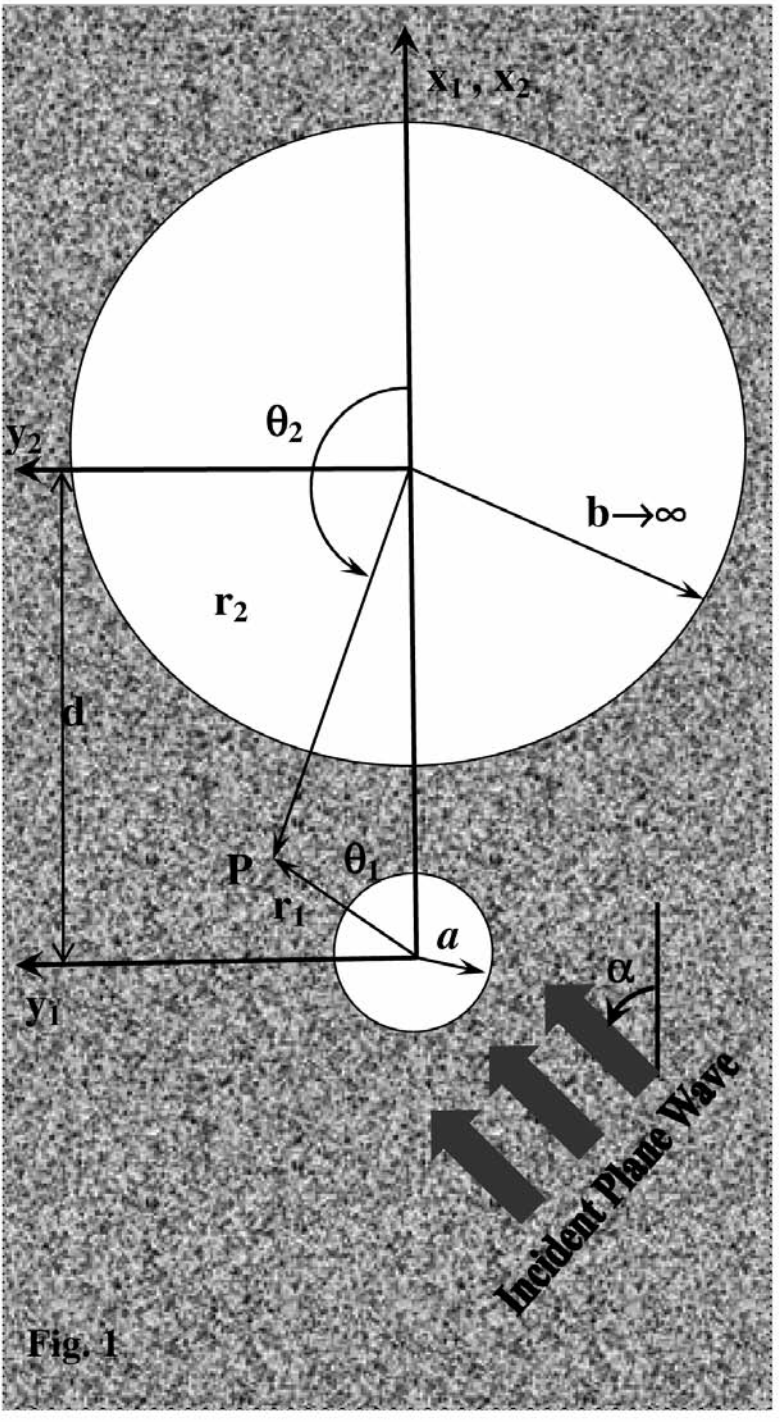

Fig. 1. Problem geometry.

Expressions for wave propagation potentials in the poroelastic medium shown in Fig. 1 are obtained by linear superposition of the incident and the reflected potential as:

$$\phi_M = \phi_f^{(i)} + \phi_s^{(i)} + \phi_f^{(j)} + \phi_s^{(j)} + \phi_{inc}^{(i)}$$

$$= \sum_{n=-\infty}^{\infty} [A_n^{(i)} H_n(k_f r_i) + B_n^{(i)} H_n(k_s r_i) + \Omega_n^{(i)} J_n(k_{inc} r_i)] e^{in\theta_i}$$

$$+ \sum_{n=-\infty}^{\infty} [A_n^{(j)} H_n(k_f r_j) + B_n^{(j)} H_n(k_s r_j)] e^{in\theta_j} \quad ,$$

$$\psi_M = \psi^{(i)} + \psi^{(j)} = \sum_{n=-\infty}^{\infty} [C_n^{(i)} H_n(k_t r_i)] e^{in\theta_i} + \sum_{n=-\infty}^{\infty} [C_n^{(j)} H_n(k_t r_j)] e^{in\theta_j} \quad , \qquad (18)$$

where i,j = 1,2, i ≠ j. In eq. (18), the scattered field from each cavity is expressed in the coordinate system centered at the same cavity. To impose the boundary conditions on the surface of i-th cavity, the j-th cavity contribution has to be transformed to the i-th cavity coordinate system. This is accomplished through the application of the Graf's addition theorem (Abramovitz and Stegun, 1964) for the cylindrical Hankel functions:

$$H_n(kr_j) e^{in\theta_j} = \sum_{m=-\infty}^{\infty} H_{n-m}(kd_{ji}) J_m(kr_i) e^{i(n-m)\theta_{ji} + im\theta_i} \quad , \quad d_{ji} > r_i \qquad (19)$$

where d_{ji} is the distance between the z-axes of the two systems, while θ_{ji} is the angle between the positive semi-axis x_j and d_{ji}. Incorporation of the above addition theorem in eq. (18) allows us to write it in the following form:

$$\phi_M(r_i, \theta_i) = \sum_{n=-\infty}^{\infty} [A_n^{(i)} H_n(k_f r_i) + B_n^{(i)} H_n(k_s r_i) + \Omega_n^{(i)} J_n(k_{inc} r_i)] e^{in\theta_i}$$

$$+ \sum_{n=-\infty}^{\infty} \sum_{m=-\infty}^{\infty} [A_m^{(j)} J_n(k_f r_i) a_{mn} + B_m^{(j)} J_n(k_s r_i) b_{mn}] e^{in\theta_i} \quad ,$$

$$\psi_M(r_i,\theta_i) = \sum_{n=-\infty}^{\infty} [C_n^{(i)} H_n(k_t r_i)] e^{in\theta_i} + \sum_{n=-\infty}^{\infty} \sum_{m=-\infty}^{\infty} [C_m^{(j)} J_n(k_t r_i) c_{mn}] e^{in\theta_i} \quad , \qquad (20)$$

where

$$a_{mn} = H_{m-n}(k_f d) e^{i(m-n)\theta_{ji}} \quad ,$$

$$b_{mn} = H_{m-n}(k_s d) e^{i(m-n)\theta_{ji}} \quad ,$$

$$c_{mn} = H_{m-n}(k_t d) e^{i(m-n)\theta_{ji}} \quad . \qquad (21)$$

It is requisite that the following boundary conditions on the surface of each cavity be satisfied:

$$\sigma_{rr}^{(i)}\big|_{r_i=a_i} = 0 \quad ,$$

$$\sigma_{r\theta}^{(i)}\big|_{r_i=a_i} = 0 \quad ,$$

$$\dot{w}_r^{(i)}\big|_{r_i=a_i} = \kappa_s p_p^{(i)}\big|_{r_i=a_i} \quad , \qquad (22)$$

where $\dot{w}_r = \phi_0(\dot{U}_r - \dot{w}_r)$ is the filtration velocity and κ_s characterizes the permeability of the interface. Applying the boundary conditions (22), after some manipulations, leads to the linear system of equations:

$$AX = B_{inc} \quad ; \quad B_{inc} = B_P, B_{SV} \qquad (23)$$

where A is a (12N + 6) by (12N + 6) complex matrix (N is the truncation number), and X and B_{inc} are complex vectors. The matrix A and vector B are defined as:

$$A = [T^{xy}]_{6\times 6} \quad , \quad B_{inc} = [Q_{inc}^{11}\ Q_{inc}^{21}\ Q_{inc}^{31}\ Q_{inc}^{41}\ Q_{inc}^{51}\ Q_{inc}^{61}]^T \quad ,$$

where

$$T^{xy} = [T_{pq}^{xy}]_{(2N+1)\times(2N+1)} \quad , \quad Q_{inc}^{x1} = [Q_{inc}^{x1}\ \ ]_{(2N+1)\times 1} \quad . \qquad (24)$$

In the matrix equation, x and y range from 1 to 6 while p and q range from 1 to N. From this matrix equation, the complex coupled coefficients can be solved. To express the boundary conditions more conveniently, the following quantities are introduced:

$$K_1^{(i)}(k_{f,s}r) = k_{f,s}^2[a_{f,s}Z_n^{(i)}(k_{f,s}r) + 2\mu Z_n^{(i)''}(k_{f,s}r)] \ ,$$

$$K_2^{(i)}(k_t r) = (2i\mu n/r^2)[rk_t Z_n^{(i)'}(k_t r) - Z_n^{(i)}(k_t r)] \ ,$$

$$K_3^{(i)}(k_{f,s}r) = 2in[rk_{f,s}Z_n^{(i)'}(k_{f,s}r) - Z_n^{(i)}(k_{f,s}r)] \ ,$$

$$K_4^{(i)}(k_t r) = -n^2 Z_n^{(i)}(k_t r) + rk_t Z_n^{(i)'}(k_t r) - r^2 k_t^2 Z_n^{(i)''}(k_t r) \ ,$$

$$K_5^{(i)}(k_{f,s}r) = i\omega\phi_0(1 - \mu_{f,s})k_{f,s}Z_n^{(i)'}(k_{f,s}r) - \kappa_s Mb_{f,s}k_{f,s}^2 Z_n^{(i)}(k_{f,s}r) \ ,$$

$$K_6^{(i)}(k_t r) = \omega n\phi_0(\alpha_0 - 1)Z_n^{(i)}(k_t r)/r \ , \qquad (25)$$

where $Z_n^{(1)} = H_n^{(1)}$, $Z_n^{(2)} = J_n$. Now, using the above expressions, we may specify the elements of matrix A and vector B as:

$$T_{pq}^{(11)} = \delta_{pq}K_1^{(1)}(k_f a_i)\big|_{i=1} \quad (= T_{pq}^{(44)} \text{ if } i = 2) \ ,$$

$$T_{pq}^{(12)} = \delta_{pq}K_1^{(1)}(k_s a_i)\big|_{i=1} \quad (= T_{pq}^{(45)} \text{ if } i = 2) \ ,$$

$$T_{pq}^{(13)} = \delta_{pq}K_2^{(1)}(k_t a_i)\big|_{i=1} \quad (= T_{pq}^{(46)} \text{ if } i = 2) \ ,$$

$$T_{pq}^{(14)} = a_{mn}K_1^{(2)}(k_f a_i)\big|_{i=1} \quad (= T_{pq}^{(41)} \text{ if } i = 2) \ ,$$

$$T_{pq}^{(15)} = b_{mn}K_1^{(2)}(k_s a_i)\big|_{i=1} \quad (= T_{pq}^{(42)} \text{ if } i = 2) \ ,$$

$$T_{pq}^{(16)} = c_{mn}K_2^{(2)}(k_t a_i)\big|_{i=1} \quad (= T_{pq}^{(43)} \text{ if } i = 2) \ , \qquad (26)$$

$$T_{pq}^{21} = \delta_{pq}K_3^{(1)}(k_f a_i)\big|_{i=1} \quad (= T_{pq}^{(54)} \text{ if } i = 2) \ ,$$

$$T_{pq}^{22} = \delta_{pq}K_3^{(1)}(k_s a_i)\big|_{i=1} \quad (= T_{pq}^{(55)} \text{ if } i = 2) \ ,$$

$$T_{pq}^{23} = \delta_{pq}K_4^{(1)}(k_t a_i)\big|_{i=1} \quad (= T_{pq}^{(56)} \text{ if } i = 2) \ ,$$

$$T_{pq}^{24} = a_{mn}K_3^{(2)}(k_f a_i)\big|_{i=1} \quad (= T_{pq}^{(51)} \text{ if } i = 2) \ ,$$

$$T_{pq}^{25} = b_{mn}K_3^{(2)}(k_s a_i)\big|_{i=1} \quad (= T_{pq}^{(52)} \text{ if } i = 2) \ ,$$

$$T_{pq}^{26} = c_{mn}K_4^{(2)}(k_t a_i)\big|_{i=1} \quad (= T_{pq}^{(53)} \text{ if } i = 2) \ , \qquad (27)$$

$$
\begin{aligned}
T_{pq}^{31} &= \delta_{pq} K_5^{(1)}(k_f a_i)\big|_{i=1} \quad (= T_{pq}^{(64)} \text{ if } i = 2) \ , \\
T_{pq}^{32} &= \delta_{pq} K_5^{(1)}(k_s a_i)\big|_{i=1} \quad (= T_{pq}^{(65)} \text{ if } i = 2) \ , \\
T_{pq}^{33} &= \delta_{pq} K_6^{(1)}(k_t a_i)\big|_{i=1} \quad (= T_{pq}^{(66)} \text{ if } i = 2) \ , \\
T_{pq}^{34} &= K_5^{(2)}(k_f a_i) a_{mn}\big|_{i=1} \quad (= T_{pq}^{(61)} \text{ if } i = 2) \ , \\
T_{pq}^{35} &= K_5^{(2)}(k_s a_i) b_{mn}\big|_{i=1} \quad (= T_{pq}^{(62)} \text{ if } i = 2) \ , \\
T_{pq}^{36} &= K_6^{(2)}(k_t a_i) c_{mn}\big|_{i=1} \quad (= T_{pq}^{(63)} \text{ if } i = 2) \ ,
\end{aligned} \tag{28}
$$

$$
\begin{aligned}
Q_{P_{p1}}^{11}(k_f a_i) &= -K_1^{(2)}(k_f a_i)\Omega_n^{(i)}\big|_{i=1} \quad (= Q_{P_{p1}}^{41} \text{ if } i = 2) \ , \\
Q_{P_{p1}}^{21}(k_f a_i) &= -K_3^{(2)}(k_f a_i)\Omega_n^{(i)}\big|_{i=1} \quad (= Q_{P_{p1}}^{51} \text{ if } i = 2) \ , \\
Q_{P_{p1}}^{31}(k_f a_i) &= -K_5^{(2)}(k_f a_i)\Omega_n^{(i)}\big|_{i=1} \quad (= Q_{P_{p1}}^{61} \text{ if } i = 2) \ ,
\end{aligned} \tag{29}
$$

$$
\begin{aligned}
Q_{SV_{p1}}^{11}(k_t a_i) &= -K_2^{(2)}(k_t a_i)\Omega_n^{(i)}\big|_{i=1} \quad (= Q_{SV_{p1}}^{41} \text{ if } i = 2) \ , \\
Q_{SV_{p1}}^{21}(k_t a_i) &= -K_4^{(2)}(k_t a_i)\Omega_n^{(i)}\big|_{i=1} \quad (= Q_{SV_{p1}}^{51} \text{ if } i = 2) \ , \\
Q_{SV_{p1}}^{31}(k_t a_i) &= -K_6^{(2)}(k_t a_i)\Omega_n^{(i)}\big|_{i=1} \quad (= Q_{SV_{p1}}^{61} \text{ if } i = 2) \ ,
\end{aligned} \tag{30}
$$

where $n = p - N - 1$, $m = q - N - 1$ and δ_{pq} is Kronecker's symbol. The variable of interest (i.e., hoop stress) is defined by eq (17). After some algebraic simplifications this expression may be written in the form:

$$
\begin{aligned}
\sigma_{\theta\theta}(r_i,\theta_i) &= \sigma_{\theta\theta}^{(\mathrm{Inc-P,SV})} \\
&+ \sum_{n=-\infty}^{\infty} A_n^{(i)}[(a_f k_f^2 - 2\mu n^2/r_i^2)H_n(k_f r_i) + 2\mu(k_f/r_i)H_n'(k_f r_i)]e^{in\theta_i} \\
&+ C_n^{(i)}(2\mu i n^2/r_i^2)[H_n(k_t r_i) - r_i k_t)H_n'(k_t r_i)]e^{in\theta_i} \\
&+ B_n^{(i)}[(a_s k_s^2 - 2\mu n^2/r_i^2)H_n(k_s r_i) + 2\mu(k_s/r_i)H_n'(k_s r_i)]e^{in\theta_i}
\end{aligned}
$$

$$+\sum_{n=-\infty}^{\infty}\sum_{m=-\infty}^{\infty} A_m^{(j)}[(a_f k_f^2 - 2\mu n^2/r_i^2)J_n(k_f r_i) + 2\mu(k_f/r_i)J_n'(k_f r_i)]a_{mn}e^{in\theta_i}$$

$$+ B_m^{(j)}[(a_s k_s^2 - 2\mu n^2/r_i^2)J_n(k_s r_i) + 2\mu(k_s/r_i)J_n'(k_s r_i)]b_{mn}e^{in\theta_i}$$

$$+ C_m^{(j)}(2\mu i n^2/r_i^2)[J_n(k_t r_i) - r_i k_t J_n'(k_t r_i)]c_{mn}e^{in\theta_i} \quad , \tag{31}$$

where

$$\sigma_{\theta\theta}^{(\mathrm{Inc-P})} = \sum_{n=-\infty}^{\infty}(a_f k_f^2 - 2\mu n^2/r_i^2)J_n(k_f r_i) + 2\mu(k_f/r_i)J_n'(k_f r_i)\Omega_n^{(i)}e^{in\theta_i} \quad ,$$

$$\sigma_{\theta\theta}^{(\mathrm{Inc-SV})} = \sum_{n=-\infty}^{\infty}(2\mu i n^2/r_i^2)[J_n(k_t r_i) - r_i k_t J_n'(k_t r_i)]\Omega_n^{(i)}e^{in\theta_i} \quad . \tag{32}$$

This completes the necessary background required for the closed form analysis of a pair of cylindrical cavities. Following the procedure described above, one can evaluate quantitatively the amplification and reduction of the stresses during the dynamic P- and SV-waves-tunnel interaction process. Next we consider some numerical examples.

NUMERICAL RESULTS

The scattered field around an underground tunnel is distorted when the tunnel is located close to the ground surface. Considering Fig. 1, in order to model a Tunnel 1 with radius a located close to a flat boundary of a ground surface, the radius b of Tunnel 2 is set to be sufficiently large. Therefore, in the analysis, b/a is tended to infinity by setting b/a = 100 (Davis et al., 2001). Considering practical applications, we set a = 3.5 m. To illustrate the effects of the ground surface on the stresses around Tunnel 1, the results are compared to those obtained without considering the flat boundary.

The Biot theory accounts for the dissipation of the propagating waves in a poroelastic medium and is used to calculate a realistic estimate of the stresses around Tunnel 1. The input parameter values for water-saturated Ridgefield sandstone, which are used to characterize the poroelastic medium, are compiled in Table 1 from Johnson et al. (1994). Moreover, the results are compared to those obtained for an equivalent elastic medium to illustrate deviation of the scattering phenomenon in poroelasticity from the classical elastic case. To do this, we determine the elastic constants for the elastic medium so as to give

dynamic properties as close as possible to the Biot medium. We accomplish this by making the elastic compressional wave speed [$c_L = \sqrt{(\lambda_e + 2\mu_e/\rho_e)}$] equal to the Biot fast wave speed; by making the shear wave speed [$c_T = \sqrt{(\mu_e/\rho_e)}$] in the elastic medium equal to that in the Biot medium; and by making the elastic density equal to the average static density in the Biot medium.

For the current problem and using the values tabulated in Table 1, smaller than the Biot critical frequency $f_c = \phi_0\eta/2\pi\rho_{fl}\kappa\alpha = 1.33 \times 10^3$ Hz, there are two other crossover frequencies; first, a frequency $f_x = 2.3$ Hz at which the wavelengths become comparable to the size of the Tunnel 1 and second, a frequency where fluid diffusion length is of the order of the diameter of Tunnel 1 $f_0 = \kappa K_f/\eta\phi_0 a^2 = 0.13$ Hz (Gurevich et al., 1998). The latter peak frequencies depend on the size of the tunnel a and always are much smaller than the Biot critical frequency. The primary idea of this research is to study the presence of the boundary of a half space and its effects on the scattered wave field, hence, a frequency band $0.1 < f < 10$ Hz is chosen.

Table 1. Input parameter values used in Biot's model.

Parameter	Water-Saturated Sandstone
ϕ_0	0.37
α_∞	1.58
κ (m^2)	27.7×10^{-12}
ρ_s (Kg/m^3)	2480
K_s (N/m^2)	4.99×10^{10}
K_o (N/m^2)	5.24×10^9
μ (N/m^2)	3.26×10^9
ρ_{fl} (Kg/m^3)	1000
K_{fl} (N/m^2)	2.25×10^9
η (Kg/m·sec)	0.1
Λ (m)	19.4×10^{-6}

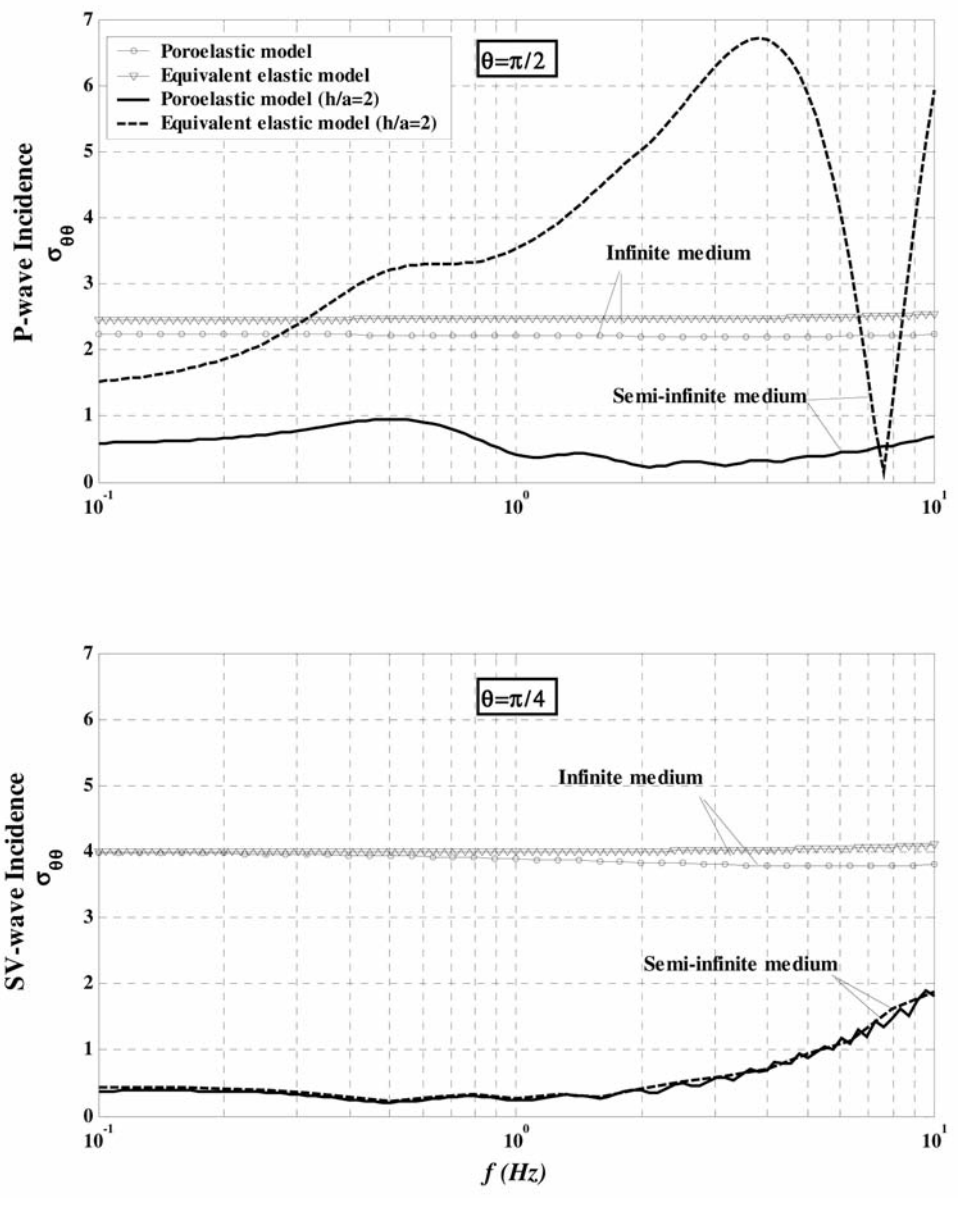

Fig. 2. Circumferential stress $\sigma_{\theta\theta}$ versus frequency, for wave incidence on an unlined cylindrical cavity in semi-infinite h/a = 2 (solid and dashed lines) and infinite h/a = ∞ (circles and triangles) poroelastic (circles and the solid line) and equivalent elastic (triangles and the dashed line) medium with incident angle $\alpha = 0$ for (a) P-wave incidence and $\theta = \pi/2$ (b) SV-wave incidence and $\theta = \pi/4$.

Fig. 2 shows the circumferential stress $\sigma_{\theta\theta}$ on the wall of the tunnel (r=a) at different frequencies, and for two cases where the incident P- and SV-waves propagate perpendicularly ($\alpha = 0$) to the free surface, impinging the tunnel from its bottom. Two different angles $\theta = \pi/2$ and $\theta = \pi/4$ are considered for P- and SV-wave incident cases. The reason can be explained by a brief look at Fig. 3, which shows that peaks occur with $\pi/4$ lag for the P and the SV incidence cases.

In Fig. 2, the effects of the slow compressional waves as well as the effects of the overburden thickness are considered for a tunnel embedded in a semi-infinite (h/a = 2) and an infinite (h/a $\rightarrow \infty$) poroelastic and equivalent elastic medium. Fig. 2(a) considers compressional wave incidence on the cavity and well exhibits the attenuation of the fast compressional wave due to mode conversion into Biot's slow wave (Ciz et al., 2006). This attenuation is significant at frequencies close to the scattering peak frequency where the wavelengths become comparable to the size of the tunnel (f_x = 2.3 Hz), and for small overburden thicknesses (h/a = 2), where there is multiple-scattering of waves between Tunnel 1 and the ground surface (Ciz et al., 2006).

In the case of the infinite medium, the difference between the poroelastic model and the equivalent elastic model is decreased, but still is noticeable. Therefore, considering the substantial difference between the semi-infinite poroelastic model and the other models shown in Fig. 2(a), the other models may result into over estimations.

Fig. 2(b) shows a major difference between infinite and semi-infinite models. This is mainly because the reflected waves from the free surface reduce the effect of the incident wave more strongly, so relatively thinner overburden renders a smaller stress concentration factor particularly at lower frequencies as the h becomes smaller in comparison with the wavelength. In the other hand at a constant magnitude of h/a, an increase in frequency, will result in relatively thicker overburden and greater overall magnitude of hoop stress around the cavity. Here one should notice this over estimation again which arises from infinite medium modeling of the problem.

Fig. 3 illustrates the changes of $\sigma_{\theta\theta}$ around the wall of Tunnel 1 (r = a) for P- and SV-wave incidences perpendicularly to the free surface ($\alpha = 0$) at frequencies 1 and 10 Hz. The ratio h/a is equal to 2, and 10 as shown. This figure reveals that in the low frequency range, a greater value of h/a, i.e., relatively thicker overburden, renders a larger value for $\sigma_{\theta\theta}$. The reason is that the reflected waves downward to the medium from the free surface do not cancel out the effect of the incident wave as strong as they do in the thinner overburden case. The latter effect is quite visible in case of the SV-wave incident.

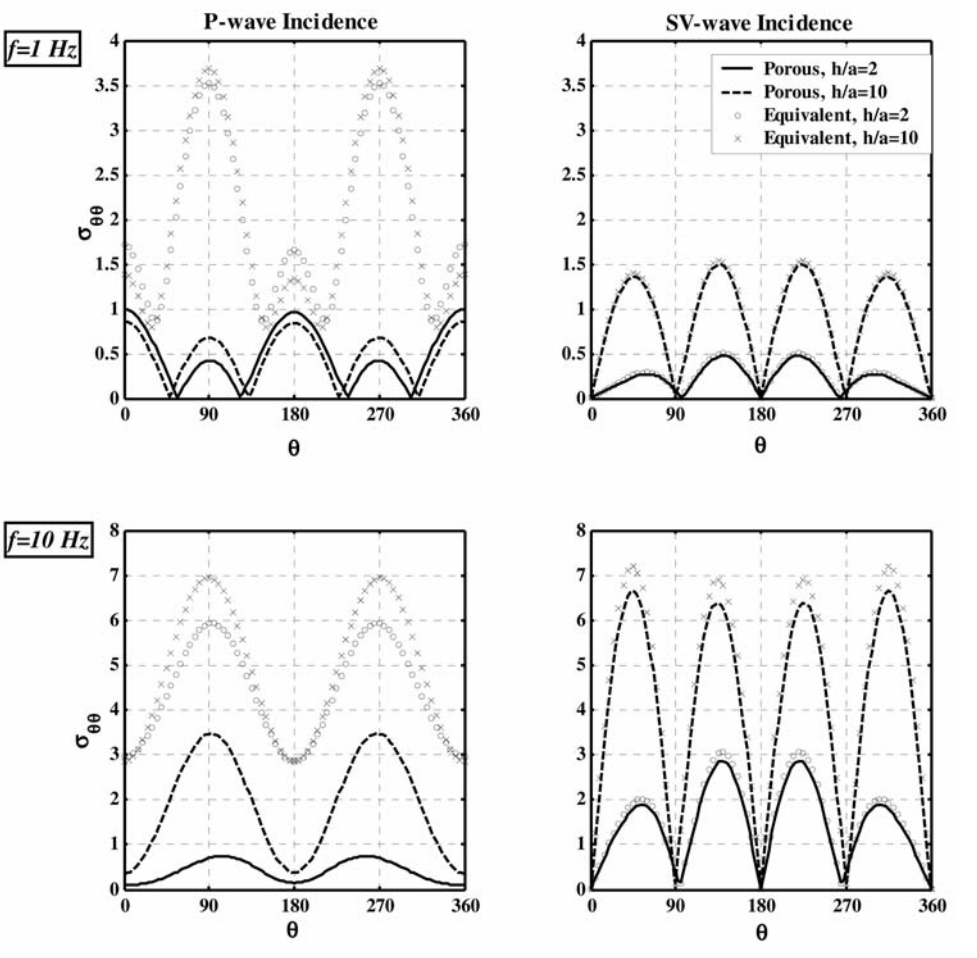

Fig. 3. Circumferential stress $\sigma_{\theta\theta}$ versus angle, for wave incidence on an unlined cylindrical cavity in semi-infinite h/a = 2 (the solid line and circles) and h/a = 10 (the dashed line and crosses) poroelastic (the solid and dashed lines) and equivalent elastic (circles and crosses) medium with incident angle $\alpha = 0$ for frequencies 1 and 10 Hz.

Fig. 3 confirms that while overburden thickness exhibits its effects clearly in the case of the SV-wave incidence; effects of mode conversion from fast to slow compressional waves becomes quite visible in the P wave incident case. Also, in the P-wave incidence case, the figure shows that the location of the peak values of $\sigma_{\theta\theta}$ translates to sidewalls from ceiling and bottom of the tunnel

as the frequency increases from 1 to 10 Hz. In the case of SV-wave incidence, the locations of the peak values remain constant at periodic 90 degrees. Finally, in order to check the overall validity of the work, Fig. 7 of the reference 2 is regenerated using the elastic approximations in our general MATLAB routine (Fig. 4).

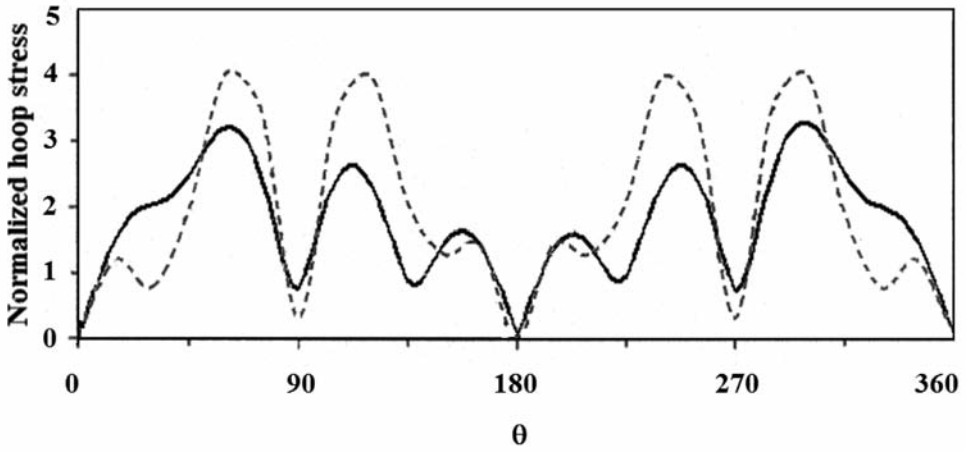

Fig. 4. Normalized hoop stress around a tunnel cavity buried in an elastic halfspace, determined by the current method (solid line) and by the method represented by Davis et al. (2001) (dashed line).

CONCLUSIONS

In this study, the dynamic behavior of a uniformly tunnel situated close to a free surface is considered based on a two-dimensional linear elastic wave analysis. Using numerical examples, the effect of the overburden thickness, Biot slow waves, and multiple-scattering are illustrated for the outlined problem. From the three existing crossover frequencies f_c, f_x and f_0, the frequency f_x at which the wavelengths become comparable to the size of the Tunnel 1 is considered to illustrate the effects of the Biot slow waves and the multiple-scattering between the tunnel and the ground surface simultaneously.

When a shear vertical incident wave propagates normal to the free surface, the magnitude of the wave being scattered around the tunnel strongly depends on the overburden thickness. This effect should be considered when

using infinite medium approximations rather than a semi-infinite model. The effects of slow waves are expendable in the case of SV-wave incidence, that is to say one can use equivalent elastic medium approximations instead of poroelastic model satisfactorily in the latter case.

A more detailed analysis including the initial static stresses, a more realistic tunnel configuration and the transient response of the tunnel are needed in the further study.

REFERENCES

Abramovitz, M. and Stegun, I.A., 1964. Handbook of Mathematical Functions. Dover Publishers, New York.

Achenbach, J.D., 1973. Wave Propagation in Elastic Solids. North-Holland Scientific Publishing Co., New York.

Allard, J.F., 1993. Propagation of Sound in Porous Media, Modeling Sound Absorbing Materials. Elsevier Applied Science, London.

Bourbie, T., Coussy, O. and Zinszner, B.E., 1987. Acoustics of Porous Media. Gulf Publishing, Houston.

Cao, H. and Lee, V.W., 1990. Scattering and diffraction of plane P waves by circular cylindrical canyons with variable depth-to-width ratio. Internat. J. Soil Dynam. and Earthq. Engin., 9: 140-150.

Chen, Z., Liu, D. and Yang, Z., 2003. Dynamic stress concentration and scattering of SH-wave by interface elliptic cylindrical cavity. Earthq. Engin. and Engin. Vibrat., 2: 299-306.

Ciz, R., Gurevich, B. and Markov, M., 2006. Seismic attenuation due to wave-induced fluid flow in a porous rock with spherical heterogeneities. Geophys. J. Int., 165: 957-968.

Davis, C.A., Lee, V.W. and Bardet, J.P., 2001. Transverse response of underground cavities and pipes to incident SV waves. Earthq. Engin. and Struct. Dynam., 30: 383-410.

Filshtinsky, M.L. and Bardzokas, D.I., 2001. The shear wave diffraction on tunnel cavities in an elastic layer and a half-layer. Archive Appl. Mechan., 71: 341-352.

Gurevich, B., Sadovnichaja, A.P., Lopatnikov, S.L. and Shapiro, S.A., 1998. Scattering of a compressional wave in a poroelastic medium by an ellipsoidal inclusion. Geophys. J. Int., 133: 91-103.

Johnson, D.L., Plona, T.J. and Kojima, H., 1994. Probing porous media with first and second sound, II. Acoustic properties of water-saturated porous media. J. Appl. Physics, 76: 115-125.

Lee, V.W. and Cao, H., 1989. Diffraction of SV waves by circular cylindrical canyons of various depths. ASCE J. Engin. Mechanics, 115: 2035-2056.

Luco, J.E. and De Barros, F.C.P., 1994. Dynamic displacements and stresses in the vicinity of a cylindrical cavity embedded in a half-space. Earthq. Engin. and Struct. Dynamics, 23: 321-340.

Morse, P.M. and Feshbach, H., 1953. Methods of Theoretical Physics. McGraw Hill, New York.

Nazarenko, A.M., 1991. Diffraction of shear waves on cylindrical inclusions and cavities in an elastic half space. Strength of Materials (English translation of Problemy Prochnosti), 22: 1669-1674.